Optical Materials 85 (2018) 86–90

Contents lists available at ScienceDirect

Optical Materials

journal homepage: www.elsevier.com/locate/optmat

Luminescent performance of $Ca_2SnO_4:Tb^{3+}$ phosphors with Li^+ co-doping

Junfeng Ma*, Yulin Chen, Xun Wang, Shanqiao Cao, Qi Chen

School of Renewable Energy, North China Electric Power University, Beijing, 102206, China

ARTICLE INFO

Keywords:
Phosphors
Solid state reaction
Point defects
Luminescence
X-ray diffraction

ABSTRACT

Long afterglow phosphors $Ca_2SnO_4:Tb^{3+}$, Li^+ with a green light were successfully synthesized by solid-state reaction, and their phase composition and luminescent property also studied using X-ray powder diffraction (XRD), photoluminescence (PL) and afterglow decay measurement. The results show that adding a small amount of Li^+ ions does not have a significant effect on the crystal structure of $Ca_2SnO_4:Tb^{3+}$, and that $Ca_2SnO_4:Tb^{3+}$, Li^+ samples are single phase of solid solutions. Their luminescent properties are strongly dependent on Li^+ doping modes. The distortion of host lattice and change of the local crystal field symmetry around Tb^{3+} enhanced their emission intensity, while the formation of oxygen vacancy and the suitable depth traps improved their afterglow performance; but the association of interstitial Li^+ (Li_i) with Ca^{2+} vacancy (V''_{Ca}), and excessive Li^+ ions would worsen their phosphorescence. Their afterglow mechanism was proposed.

1. Introduction

The green phosphors with Tb^{3+} can be widely used in many fields, such as laser projection displays, light-emitting diodes (LED), radiation detection [1–3]. In 2005, a green light $CaSnO_3:Tb^{3+}$ with 4 h afterglow time was successfully prepared for the first time [4], but long afterglow luminescent materials of alkaline earth metal stannates had been rarely reported before. Stannate materials have attracted a lot of attention due to their interesting electronic and optical properties, environment-friendly features, and easy preparing process [5,6]. Although various long lasting phosphors in which stannite was used as a matrix were reported, such as $MSnO_3$ (M = Ca, Sr, and Ba):Eu^{3+} with red luminescence [7], $CaSnO_3:Gd^{3+}$ with cyan emission [8], and $CaSnO_3:Sm^{3+}$ with the emission of orange red light [9]; few studies were involved in Ca_2SnO_4 as matrix materials, especially on improving their luminescence performance. Many efforts have been made to enhance the afterglow property of alkaline earth aluminate or silicate phosphors, e.g. by varying the added quantities of co-dopants [10] or using various fluxes [11], but there have been little researches on the stannate system. Previous studies also show that appropriately adding fluxes in phosphors can effectively reduce their synthesis temperature and improve their luminescent property [11–13], and different fluxes like H_3BO_3, Li_3PO_4, Li_2CO_3, Na_2CO_3, K_2CO_3, and MgF_2 are widely used in the preparation of various phosphors [14]. Herein, for $Ca_2SnO_4:Tb^{3+}$ phosphors, can Li_2CO_3 also enhance their afterglow performance? If so, how will it work? Actually, it can be also considered as Li^+ doping process when the added quantity of Li_2CO_3 is low. To the best of our knowledge, no such studies have been reported. Therefore, the present study is undoubtedly of important significance in revealing the influence of Li_2CO_3 addition or Li^+ doping on the photoluminescence of $Ca_2SnO_4:Tb^{3+}$ phosphors and improving their luminescent property.

2. Experimental

2.1. Synthesis of samples

$Ca_2SnO_4:Tb^{3+}$ phosphors with different doped quantity of Li^+ ions were synthesized using a solid-state reaction technique. The starting materials, $CaCO_3$, SnO_2, Tb_4O_7, and Li_2CO_3 (H_3BO_3 as another dopant for comparison) were respectively weighed out according to the nominal composition of $Ca_{1.999-m}SnO_4:Tb^{3+}_{0.001}$, Li^+_m (m = 0, 0.01, 0.03, 0.05, and 0.07, and the samples were denoted in turn as S_0, S_1, S_3, S_5, and S_7) for each sample. All the samples were thoroughly mixed for 1 h in an agate mortar before they were loaded into corundum crucibles and pre-fired at 1000 °C for 4 h in air atmosphere, and then calcined under N_2 atmosphere at 1400 °C for 4 h. After cooling, they were again ground in an agate mortar for their characterization and investigation.

2.2. Characterization of samples

The phase compositions of the synthesized samples were determined by an X-ray powder diffractometer with Cu K_α radiation (XRD, D8 Advance, Bruker, Germany), Their emission spectra and decay curves were obtained by a Hitachi F-4600 fluorescence

* Corresponding author.
E-mail address: majunfeng01@sina.cn (J. Ma).

https://doi.org/10.1016/j.optmat.2018.08.036
Received 19 June 2018; Received in revised form 13 August 2018; Accepted 15 August 2018

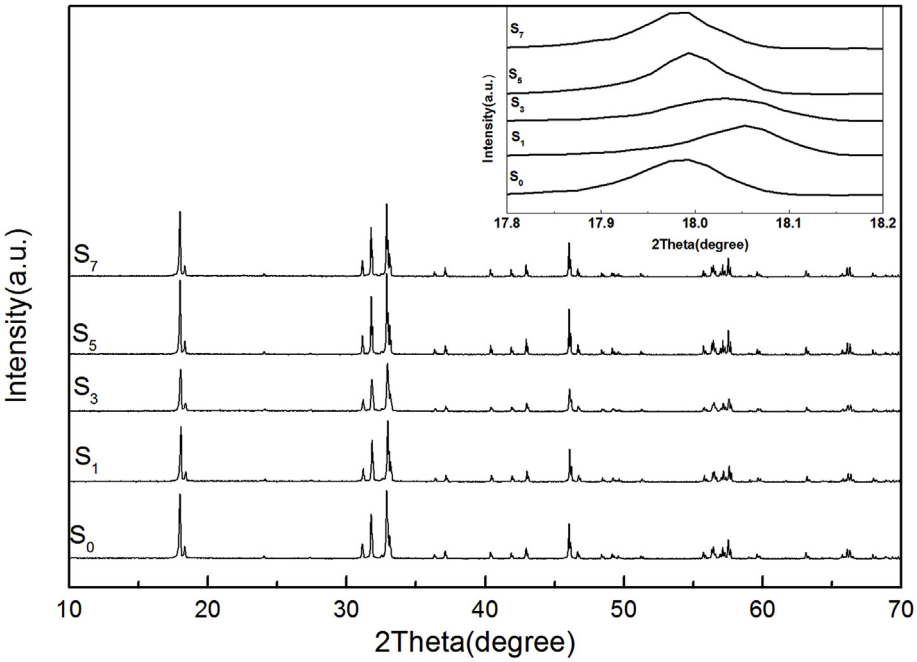

Fig. 1. XRD patterns of $Ca_2SnO_4:Tb^{3+}$ phosphors co-doped with different amounts of Li^+ ions, inset showing their magnified XRD patterns in 2θ range of 17.8°–18.2°.

spectrometer at room temperature with Xe lamp as a light source. Here, the same quantity of sample (0.50 g) was employed for each measurement. The emission wavelength scan mode was used for emission spectra (The photomultiplier voltage: 400 V, and scan speed: 240 nm/min), and time scan mode used for the decay curves (The photomultiplier voltage: 1000 V, and the excitation source by a Xe lamp at the wavelength of 255 nm for 3 min).

3. Results and discussion

The XRD patterns of as-prepared samples are shown in Fig. 1, it can be seen that all diffraction peaks for each sample are in good agreement with the standard data of Ca_2SnO_4 (JCPDS NO. 20–0241), showing a single phase, and no secondary phase can be detected. The magnified XRD patterns (inset in Fig. 1) show that their diffraction peaks slightly shift with the variation of Li^+ amounts (m value). The maximum shift of the peak position toward the higher angle side is located at m = 0.01 (S_1), then it conversely shifts toward the lower angle side with the increase of Li^+ addition from m = 0.01 to 0.05 (S_5), and no significant change can be found between 0.05 and 0.07 (S_7), and similar phenomena were also found in $La_2O_3:Er^{3+}$ phosphors [15]. The possible reason can be ascribed to different doping modes of Li^+ ions in host lattice, such as cation substitution, entering into interstitial sites [16–18]. In $Ca_2SnO_4:Tb^{3+}$, the presence of doped Tb^{3+} had introduced $Tb_{Ca}^{\cdot}$, Ca^{2+} vacancy (V_{Ca}''), Tb'_{Sn} and Sn^{3+} or Sn^{2+} ions [19–21]; herein V''_{Ca}, Tb'_{Sn}, Sn^{3+} and Sn^{2+} can act as hole trapping centers; while the defects Tb'_{Ca} may act as electron trapping centers. These trapping centers play essential roles for photoenergy storage in persistent phosphors.

In the present study, adding Li^+ in $Ca_2SnO_4:Tb^{3+}$ would result in the distortion of the host lattice. Initially, a small amount of Li^+ ions (m ≤ 0.01) would substitute Ca^{2+} ions to make the host lattice shrink, corresponding to the shift toward a higher angle side since the radius of Li^+ ($R_{Li}{}^+ = 0.076$ nm) is smaller than that of Ca^{2+} ion ($R_{Ca}{}^{2+} = 0.100$ nm) [22]. Then, with the increase of Li^+ addition (m = 0.01–0.05), partial Li^+ ions will possibly enter into interstitial sites [15–18], expanding the host lattice dimension with their XRD patterns shifting toward a lower angle side (inset in Fig. 1). Moreover, the more the amount of doped Li^+, the lower 2θ angle they will shift. Nevertheless, when Li^+ amount is beyond m = 0.05, no obvious 2θ angle shift can be found. The 2θ angle shift caused by host lattice dimension shrinkage or expansion can be well explained by Bragg's equation (2dsin θ = λ, where d is the interplanar distance, θ the diffraction angle and λ the wavelength of the X-ray) [23–25].

Fig. 2 displays the excitation and emission spectra of the different $Ca_2SnO_4:Tb^{3+}$ phosphors, all the excitation bands are centered near 250 nm; while several typical bands that locate respectively at 483, 545, 589, and 622 nm in their emission spectra can be assigned to the transitions from $^5D_4$ to ^7F_j (j = 6, 5, 4, 3) of Tb^{3+} [4,19,26]. It is noteworthy that the emission peaks near 510 nm arises from the frequency-doubled reflection. Obviously, their fluorescence intensity increases along with the increase of Li^+ quantity (up to m = 0.05), and reaches their maximum value at m = 0.05; and then decreases (e.g. S_7, m = 0.07). The unique variation of emission intensity with Li^+ amount is in fact associated with Li^+ doping modes in $Ca_2SnO_4:Tb^{3+}$. When doped with 0.01 of Li^+ or less, as analysed in Fig. 1 before, the substitution of Li^+ for Ca^{2+} shrinks the host lattice, changing the local crystal field symmetry around Tb^{3+} so as to enhance their fluorescence intensity [15,27]. When more Li^+ was added (m = 0.01–0.05), partial Li^+ ions would enter into interstitial sites to produce Li_i, expanding the host lattice. All these would distort their local crystal structure with activating the crystal field environment around Tb^{3+}, and consequently elevate their emission intensity [15–18,27–30]. It should be noted that both the substitution of Ca^{2+} ions and occupation of interstitial sites would change the local crystal field around the Tb^{3+} ions in the host lattice, favoring to break the forbidden transition, and consequently improve their emission intensity, just like the Li^+ in $Gd_2O_3:Eu^{3+}$ and $Y_3Al_5O_{12}:Er^{3+}$ [16,27]. Nevertheless, excessive Li^+ (m ≥ 0.05) will lead to the concentration quenching [15] to reduce their emission intensity (S_7). The results suggest that $Ca_2SnO_4:Tb^{3+}$ phosphors co-doped with Li^+ possess a better fluorescence property than that doped by single Tb^{3+} in a certain concentration range. They are green-emission phosphors, whose characteristic emission mainly originates from $^5D_4$-$^7F_5$ transition of Tb^{3+}, centered at 545 nm [4,19,26].

Fig. 3 presents their afterglow decay curves, which were obtained by measuring the afterglow emitted from the as-prepared samples with different concentrations of Li^+ over a time period of 60 s after exposed for 3 min under 255 nm excitation and then immediately excitation